ISSN 0036-0244, Russian Journal of Physical Chemistry A, 2016, Vol. 90, No. 7, pp. 1391–1404. © Pleiades Publishing, Ltd., 2016.

STRUCTURE OF MATTER AND QUANTUM CHEMISTRY

Vibrational Studies, NMR Analysis, Modeling of Electronic and Thermodynamical Parameters of 1,3-Bis(4-benzamido)triazene[1]

N. Ghalebsaz-Jeddi[a,*] and E. Vessally[b]

[a] *Department of Chemistry, Tabriz Branch, Islamic Azad University, Tabriz, Iran*

[b] *Department of Chemistry, Payame Noor University, Tehran, Iran*

**e-mail: ghalebsaz@iaut.ac.ir*

Received November 14, 2014; in final form, November 11, 2015

Abstract—The optimized geometry, vibrational wavenumbers, ^{1}H and ^{13}C chemical shift values of 1,3-bis(4-benzamido)triazene, BBT, in the ground state were computed with the Hartree-Fock (HF) and density functional theory method (PBE1PBE) with 6-311+G(2*d*,*p*) basis set. The harmonic vibrational wavenumbers of BBT were calculated and the scaled values were compared with the experimental FT-IR spectra. A detailed interpretation of the NMR spectra of BBT was reported. The calculated data are in reasonably good agreement with experimental measurements. Moreover, the log *P* value was estimated with ChemBioOffice Ultra 11.0, ACD/LogP, and ALOGPS programs.

Keywords: 1,3-bis(4-benzamido)triazene, IR, NMR, DFT, 6311+G(2*d*,*p*)

DOI: 10.1134/S0036024416070104

1. INTRODUCTION

1,3-Bisphenyl triazene has been synthesized by Griess [1]. This class of compounds is useful because they have different applications as intermediate compounds in organic synthesis [2], ligands in transition metal complexes [3–5], antibacterial [6–8], antileukemic [9], anticancer [10] and antitripanosomal [11] activities, fluorescence sensors [12–16], treatment of tumor diseases [17], photo-switchable materials [18–20] and selective electrodes for measurement of the trace amount of mercury ion in the water samples [21].The active site of these compounds, (N=N–NH), is responsible for the mentioned properties of the triazene molecules.

This research demonstrates and disputes the synthesis and characterization of new triazene, 1,3-bis(4-benzamido)triazene, BBT, by FT-IR and NMR spectroscopy. Moreover, we compared the experimental results with calculated data using the Hartree-Fock (HF) and density functional theory method (PBE1PBE) with 6-311+G(2*d*,*p*) basis set.

2. EXPERIMENTAL AND THEORETICAL METHODS

2.1. General Method

The melting point was determined in the equipment Gallenkamp. Elemental analysis was performed with Perkin-Elmer 2400 series II. ^{1}H and ^{13}C nuclear magnetic resonance spectra were recorded on a Bruker Avance 300 instrument (300 MHz; $CDCl_3$) with the processing software XWINNMR version 3.1. Chemical shifts are reported on δ scale relative to TMS. The room temperature Fourier transform infrared spectrum of the title compound was recorded in the region 4000–400 cm^{-1} with ±1 cm^{-1} resolution using a PerkinElmer spectrum RXI FT-IR spectrometer, utilizing KBr disc.

2.2. Synthesis

4-Aminobenzamide (2.181 g, 16.02 mmol) was dissolved in a mixture of 20 mL of concentrated HCl and 10 mL of distilled water and the system was cooled to –2°C. Then sodium nitrite (1.429 g, 16.82 mmol) was added under constant stirring. The system was neutralized to pH ~7, with sodium carbonate solution. The synthetic route is shown in Scheme 1. The yellow precipitate separated by filtration was washed with small amounts of cold water, followed by small amounts of cold ethanol and purified by column chromatography after its adsorption onto silica gel (70/230 mesh) using hexane : ethyl acetate (3 : 7) as eluent. The microcrystalline product was recrystallized from a hexane : ethyl acetate mixture (1 : 3). Yellow vitreous bar-shaped crystals were obtained by slow evaporation of the solvent mixture within five days. Yield of 86% (1.75 g, 5.7 mmol) based on taken 4-aminobenzamide, T_{mp} = 115–116°C, FT-IR, cm^{-1}, KBr pellets: 3732 (N–H, amide), 3415 (N–H, amide),

[1] The article is published in the original.

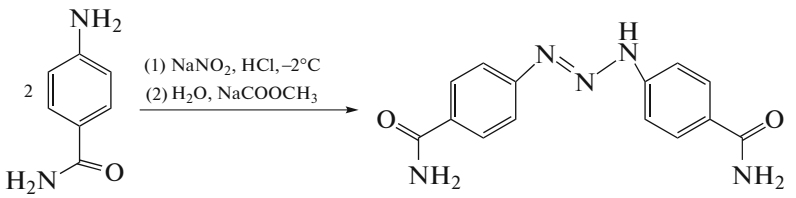

Scheme 1. Synthesis of BBT.

3323 (C–H), 3157 (C–H), 1656 (C=C), 1604 (N–H), 1525 (d(C–H), deformation), 1247 (C–N), 1053 (C–O), 743 ((C–Cl), deformation). ^{1}H NMR (300 MHz, DMSO-*d*6/tms) d 12.84 (s, 1H, NH), 7.93–7.29 (m, 8H, Ph), 3.32 (2H, NH), 3.34 (2H, NH). ^{13}C NMR (300 MHz, DMSO-*d*6) d 168 (2C=O), 154.35, 146.54, 130.99, 128.39, 128.34, 127.60, 127.60, 124.61, 120.79, 120.69, 116.45, 116.41 (Ph).

2.3. Theoretical Methods

All the calculations were carried out with Gaussian 03 [22]. The gradient corrected density functional theory (DFT/PBE1PBE) and Hartree-Fock (HF) with the standard 6-311+G(2*d*,*p*) basis set were used. The global minimum of the molecular structure of 1,3-bis(4-benzamido)triazene, BBT, was found and used for vibrational and NMR calculations. The calculated frequencies were scaled by 0.9073 and 0.9944 for HF/6-311+G(2*d*,*p*) and PBE1PBE/6-311+G(2*d*,*p*) respectively [23]. The assignments that be made are only on a base of a normal coordinate analysis. The chemical shifts were calculated by the Gaussian and ACD/NMR programs [24]. GaussSum was used to calculate group contributions to the molecular orbital and prepare the partial density of states (DOS) spectra [25].

3. RESULTS AND DISCUSSION

3.1. The Geometrical Studies

The obtained global minimum of 1,3-bis(4-benzamido)triazene, BBT, was shown in Fig. 1. The compound under investigation is rather complicated. This molecule has different degrees of hindered internal rotation and the compound can exist as a mixture of conformers with different stabilities. The number and structure of possible conformations estimated on a base of theoretical analysis. The structures of possible conformations were presented in Fig. 2. The most stable structure of conformer was selected for this discussion. In the most stable structure of conformer two carbonyl groups are *anti* and the C–NH–N=N moiety is *trans* (Fig. 1). The *cis* C–NH–N=N moiety

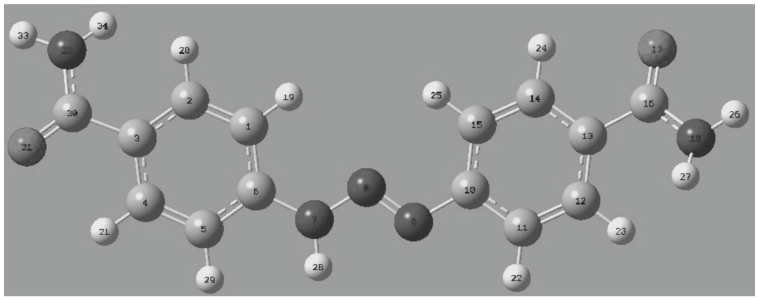

Optimized structure with RPBE1PBE/6-311+G(2*d*,*p*)

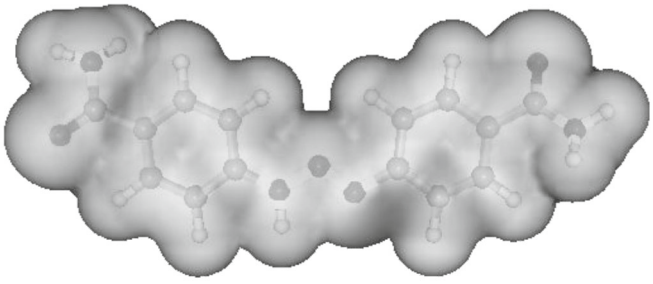

3D Molecular electrostatic potential map with RPBE1PBE/6-311+G(2*d*,*p*)

Fig. 1. Optimized structure and calculated 3D molecular electrostatic potential map for BBT at RPBE1PBE/6-311+G(2*d*,*p*) level.

Table 1. Geometrical parameters optimized in BBT, bond length (Å), bond angle (deg), and dihedral angle (deg)

Parameters	X-ray	PBE1PBE6-311+G(2*d*,*p*)	HF/6-311+G(2*d*,*p*)	Parameters	X-ray	PBE1PBE6-311+G(2*d*,*p*)	HF/6-311+G(2*d*,*p*)
Bond length				Bond angle			
C30–N32	1.335[(1)]	1.365	1.363	C16–C13–C14	118.3[(1)]	117.4	117.8
C30–O31	1.233[(1)]	1.216	1.194	C13–C14–C15	119.2[(2)]	120.9	120.8
C30–C3	1.489[(1)]	1.490	1.493	C13–C12–C11	120.5[(1)]	120.3	120.3
C16–N18	1.335[(1)]	1.365	1.361	C14–C15–C10	119.5[(2)]	119.8	119.6
C16–O17	1.233[(1)]	1.215	1.193	C15–C10–C11	119.9[(2)]	119.4	119.7
C16–C13	1.489[(1)]	1.493	1.498	C10–C11–C12	120.5[(2)]	120.3	120.2
N9–C10	1.430[(2)]	1.405	1.498	C6–C5–C4	120.3[(2)]	120.0	120.1
N9–N8	1.263[(2)]	1.251	1.214	C6–C1–C2	119.4[(2)]	119.4	119.4
N8–N7	1.340[(2)]	1.319	1.321	C5–C4–C3	120.5[(1)]	120.8	120.9
N7–C6	1.383[(2)]	1.384	1.385	C4–C3–C2	118.4[(2)]	118.5	118.2
C6–C5	1.392[(2)]	1.396	1.390	C3–C2–C1	121.7[(1)]	121.3	121.5
C5–C4	1.366[(2)]	1.379	1.373	C1–C6–C5	119.8[(2)]	119.7	119.5
C4–C3	1.375[(2)]	1.392	1.387	$a^{\ddagger}$		0.975	0.867
C3–C2	1.375[(2)]	1.393	1.385	$b^{\ddagger}$		3.278	16.21
C2–C1	1.365[(2)]	1.382	1.379	R^2		0.801	0.785
C1–C6	1.401[(2)]	1.394	1.387	Dihedral angle			
C10–C15	1.398[(2)]	1.398	1.390	C6–N7–N8–N9	177.5[(2)]	179.1	176.7
C15–C14	1.372[(2)]	1.378	1.374	C10–N9–N8–N7	−179.9[(2)]	179.3	179.3
C14–C13	1.375[(2)]	1.395	1.389	C1–C6–N7–N8	6.38[(2)]	−1.6	0.2
C13–C12	1.373[(2)]	1.392	1.382	C5–C6–N7–N8	−173.4[(2)]	178.7	−179.5
C12–C11	1.381[(2)]	1.384	1.382	C15–C10–N9–N8	2.93[(2)]	−4.6	−10.41
C11–C10	1.383[(2)]	1.392	1.380	C11–C10–N9–N8	−175.9[(2)]	176.26	170.7
$a^{\dagger}$		1.048	1.228	C2–C3–C30–N32	178.0[(2)]	15.7	17.6
$b^{\dagger}$		−0.061	−0.310	C2–C3–C30–O31	−2.3[(1)]	−162.9	−161.0
R^2		0.949	0.939	C2–C3–C4–C5	0.27[(2)]	−1.0	−1.1
Bond angle				C2–C1–C6–C5	0.74[(2)]	−0.6	−0.6
N9–N8–N7	112.3[(2)]	112.6	113.8	C6–C1–C2–C3	−1.18[(2)]	0.24	0.3
N8–N7–C6	120.0[(2)]	122.6	122.1	C6–C5–C4–C3	−0.7[(2)]	0.65	0.8
N8–N9–C10	112.1[(2)]	114.6	115.3	C4–C3–C30–N32	−2.6[(1)]	−165.3	−163
N9–C10–C15	124.1[(2)]	125.0	124.6	C4–C3–C30–O31	176.9[(1)]	16.0	17
N9–C10–C11	115.8[(2)]	115.5	115.5	C14–C13–C16–N18	178.0[(1)]	163.2	160
N7–C6–C1	120.9[(2)]	122.0	122.4	Cl2–C13–C16–N18	−2.65[(1)]	−17.9	−21
N7–C6–C5	119.1[(2)]	118.2	118.0	C14–C13–C16–O17	−2.3[(1)]	−18.0	−20
N32–C30–O31	121.0[(1)]	121.6	121.3	Cl2–C13–C16–O17	176.9[(1)]	−160.7	157.7
N32–C30–C3	119.0[(1)]	116.6	117	C15–C14–C13–C16	178.9[(1)]	−179.9	179.9
O31–C30–C3	119.8[(1)]	121.7	121.6	C15–C14–C13–C12	−0.89[(2)]	1.16	1.29
N18–C16–O17	121.0[(1)]	121.7	121.6	C15–C10–C11–C12	−1.04[(2)]	0.9	1.3
N18–C16–C13	119.0[(1)]	116.4	116.7	C10–C11–C12–C113	0.5[(2)]	−0.3	−0.6
O17–C16–C13	119.8[(1)]	121.7	121.5	C11–C12–C13–C16	0.27[(1)]	−179.4	−179
C16–C13–C12	123.1[(1)]	123.5	123.1	C11–C12–C13–C14	0.48[(2)]	−0.6	−0.6

† $R_{theo} = aR_{exp} + b$.

‡ $A_{theo} = aA_{exp} + b$.

(1) 1-(2-Fluorophenyl)-3-(4-amidophenyl)triazene.

(2) 1,3-Bis(4-nitrophenyl)triazene.

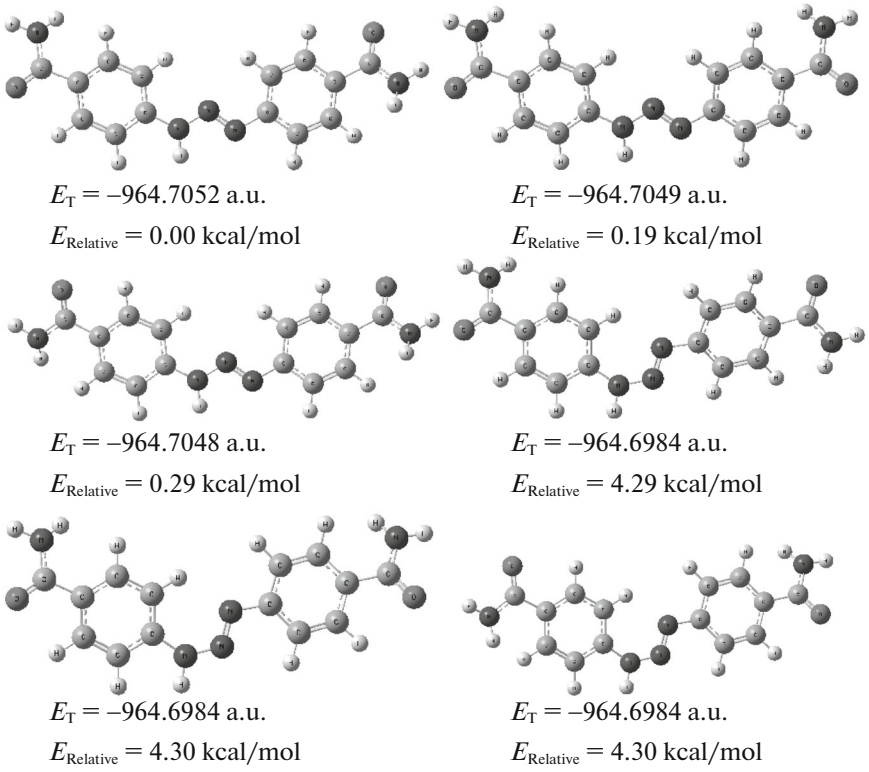

Fig. 2. Optimized structure, total energies, and relative energies for BBT at RPBE1PBE/6-311+G(2*d*,*p*) level.

leads an unstable conformer. The other hindered internal rotation such as carbonyl groups or amino groups' rotation slightly change the stability of the conformers. The geometrical parameters including bond length, bond angle and dihedral angles were presented in Table 1. Since the crystal structure of BBT is not available, the optimized structure was compared with other similar optimized compounds [26, 27]. The molecule contains two CO–NH_2 groups and triazeno moiety with two benzene rings. The theoretical amounts of the optimized bond lengths are slightly larger than the experimental amounts because the theoretical calculations belong to the isolated molecule in the gas-phase while the experimental results belong to the molecule in the solid state. Theoretical calculations on the bond angles and bond lengths at the RPBE1PBE level of theory indicated a good correlation with the experimental data compared to HF level of theory. For instance, the optimized bond length of C–C in the phenyl ring occurs in the range of 1.398–1.378 Å at the RPBE1PBE method and 1.390–1.373 Å at the HF method. This is in good agreement with an analogous molecule where the C–C bond length occurs in the range of 1.401–1.365 Å. According to the experimental values, order of the optimized bond length of the six C–C bonds in the ring are as C1–C2 < C4–C5 < C2–C3 = C3–C4 < C5–C6 < C6–C1. For the calculated RPBE1PBE values, the order of the bond lengths was slightly deviated as C5–C6 (1.396 Å) > C1–C6 (1.394 Å) > C2–C3 (1.393 Å) > C3–C4 (1.392 Å) > C1–C2 (1.382 Å) > C4–C5 (1.379 Å) (Table 1). Moreover, the predicted bond lengths of C30–O31, C16–O17 and C30–C3, C16–C13 are 1.216, 1.215 and 1.490, 1.493 Å with RPBE1PBE method; the same bond length are 1.194, 1.193 and 1.493, 1.498 Å with HF method and the experimental data of named bond are, respectively, 1.233, 1.233 and 1.489, 1.489 Å. The optimized N–C bond lengths of (N7–C6) and (N9–C10) are 1.384 and 1.405 Å, (N18–C16) and (N32–C30) are 1.365 and 1.365 Å, using RPBE1PBE method while they are 1.384, 1.405, 1.361, 1.363, respectively, using HF method. However, these are slightly different compared to a related molecular structure. The calculated C6–N7–N8 and C10–N9–N8 bond angles are 122.6° and 114.6° at RPBE1PBE and at HF method are 122.1° and 115.3°, respectively, which are 2.5° deviated from experimental data for both of the bond angles. The comparative graphs of geometrical parameters including the bond lengths, bond angles and dihedral angles of BBT for different methods were illustrated in Fig. 3.

3.2. FT-IR Spectroscopy

The title compound consists of 34 atoms, therefore it has 96 normal modes of vibration. Of the 96 normal modes of vibrations, 63 modes of vibration are in the plane and remaining 34 are out of plane. The bands that are in the plane of the molecule are represented as A' and out-of-plane as A''. Thus the 96 normal modes

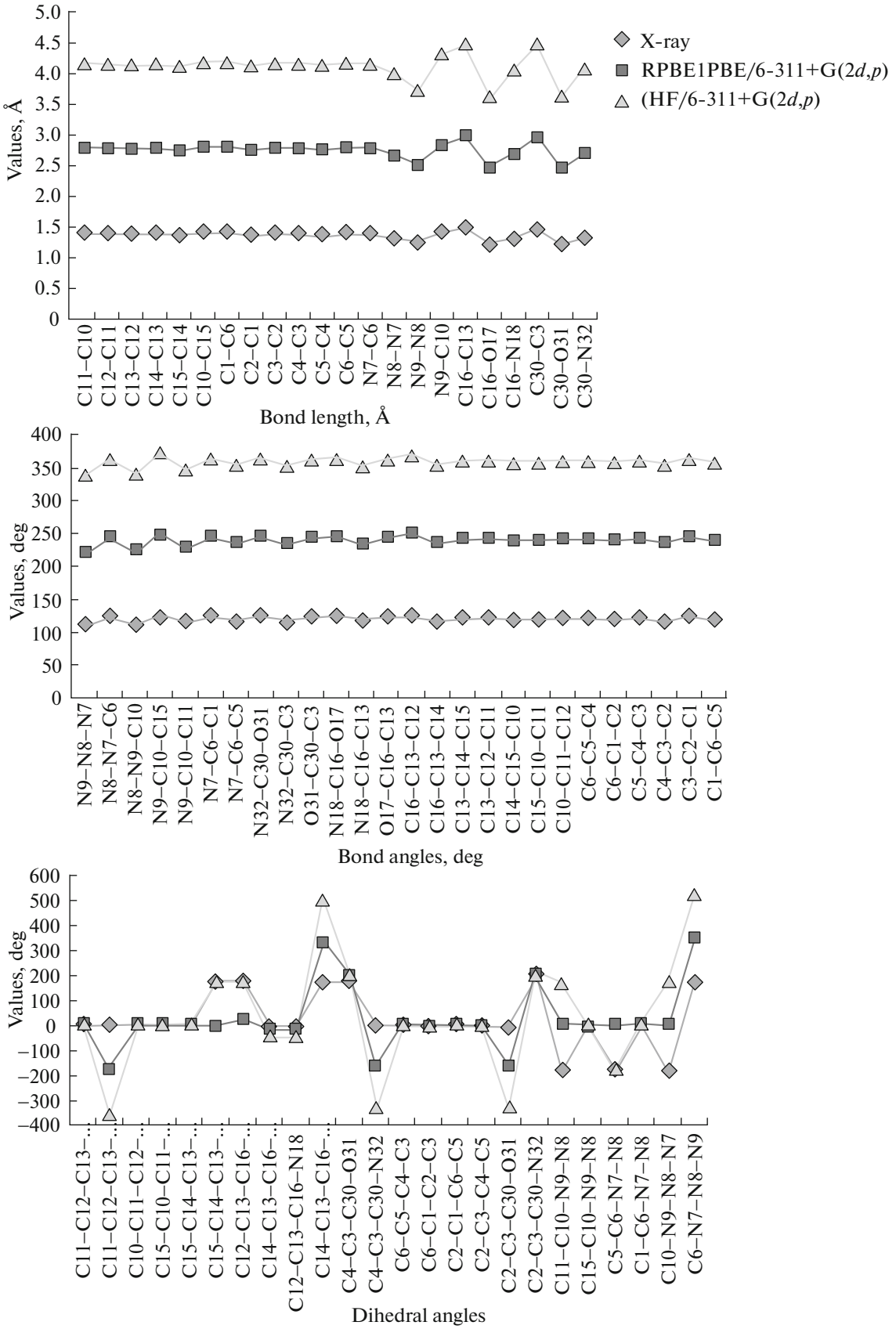

Fig. 3. Bond length, bond angle, and dihedral angle differences of 1,3-bis(4-amidophenyl)triazene between X-ray and theoretical approaches [HF/DFT], X-ray, RPBE1PBE/6-311+G(2*d*,*p*), (HF/6-311+G(2*d*,*p*) levels.

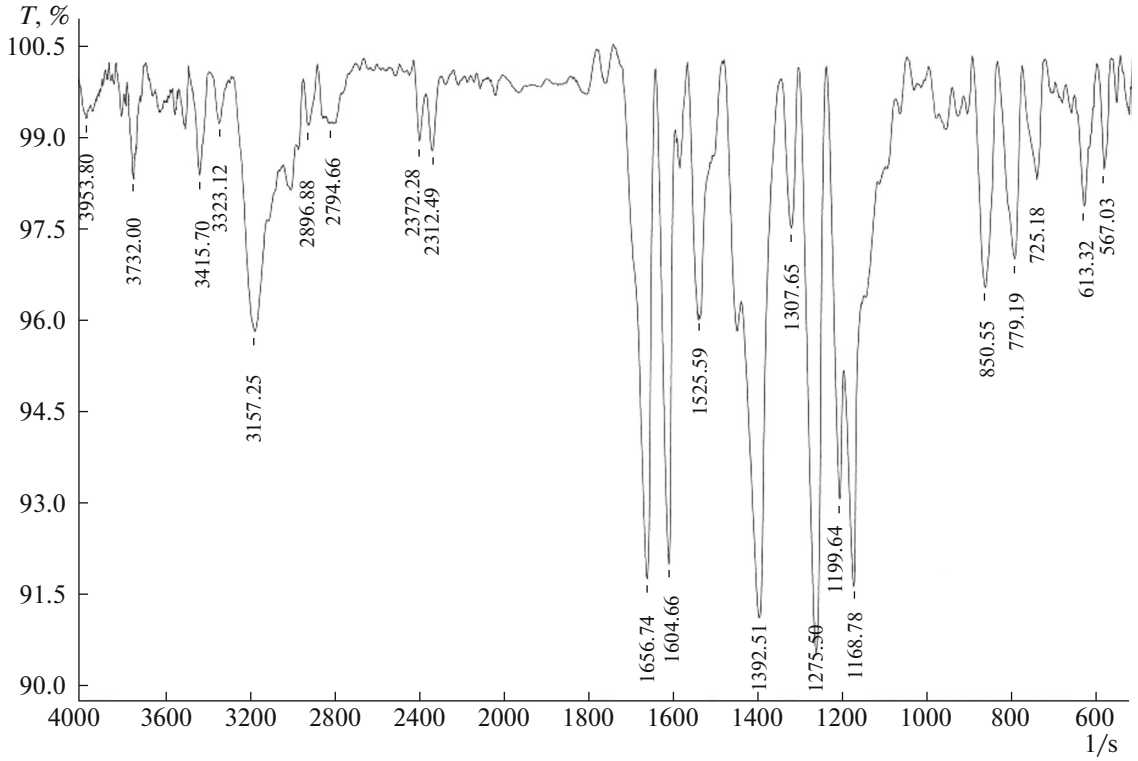

Fig. 4. FT-IR spectrum of 1,3-bis(4-amidophenyl)triazene.

of vibration of BBT are distributed as Γ_{Vib} = 61A' + 34A''. In agreement with C_S symmetry all the 96 fundamental vibrations are not active in IR absorption. The harmonic-vibrational frequencies were calculated for BBT at HF and DFT (PBE1PBE) levels using the triple split valence basis set along with the diffuse and polarization functions, 6-311+G(2*d*,*p*). The experimental FT-IR spectra are shown in Fig. 4. Observed FT-IR frequencies for various modes of vibration concerning the assignment have been presented in the Table 2. Comparison of frequencies calculated at HF with the experimental values shows overestimation of the calculated vibrational state due to the inattention of anharmonicity in the real system. Since Density functional theory includes electron correlation, certain extends make the frequency value smaller than the HF frequency data. For comparison with the experiments based on the calculations, correlation graphics are presented in Fig. 5. As shown in Fig. 5, PBE1PBE/6-311+G(2*d*,*p*) values show better agreement with the experimental values.

3.2.1. C–H vibrations. The aromatic structure displays the presence of the C–H stretching vibrations in the region 3000–3100 cm^{-1} which is the characteristic region for the ready identification of the C–H stretching vibrations [28, 29]. In this region, the bands are not considerably affected by the nature of the substituent. The wavenumber 3323 and 3157 cm^{-1} are assigned to C–H stretching vibration of the phenyl groups. These peaks are predicted at 3217 and 3166 cm^{-1} (for PBE1PBE/6-311+G(2*d*,*p*)) and 3066 and 3013 cm^{-1} (for HF/6-311+G(2*d*,*p*)) (mode no. 6.13). As indicated by the PED, these modes involve the contribution of 96 and 95%.

The scaled vibrations by PBE1PBE/6-311+G(2*d*,*p*) method show very good agreement with recorded spectral data. The aromatic C–H in-plane bending and out-of-plane bending vibrations naturally occur in the region 300–1000 and 750–1000 cm^{-1}, respectively, [30, 31]; the bands are sharp but have been weak-to medium intensity. In present case, the in-plane bending of phenyl ring computed at 1533, 1317, 1191, and 1179 cm^{-1} (for PBE1PBE/6-311+G(2*d*,*p*) matches with 1525, 1307, 1199, and 1168 cm^{-1} in IR spectrum (mode no. 24, 33, 37, 38). The PED, these modes involve the contribution of 17, 26, 28, and 28%. This C–H in-plane bending vibration shows good agreement with literature data [32–34]. The C–H vibration bands are in the expected region with relatively strong intensity, hence there is a benzene structure.

3.2.2. C=C vibrations. Generally, the ring stretching vibrations (C=C) are observed at 1625–1590, 1590–1575, 1540–1470, 1465–1430, and 1380–1280 cm^{-1} [35, 36]. Since the present molecule consists of two benzene rings, there are six C=C and stretching vibrations. The observed frequency for BBT

Table 2. Observed, PBE1PBE/6-311+G(2*d*,*p*) and HF /6-311+G(2*d*,*p*) level calculated vibrational frequencies of BBT

No.	Symmetry species C_S	Observed frequency	Calculated frequency				Vibrational assignments	PED, %
		FT-IR	PBE1PBE/6-31+G(2*d*,*p*)		HF/6-311+G(2*d*,*p*)			
			unscaled	scaled	unscaled	scaled		
1	A'	–	3745	3724	3930	3565	(N–H) υ	58
2	A'	3732m	3744	3723	3927	3562	(N–H) υ	58
3	A'	–	3618	3597	3806	3453	(N–H) υ	54
4	A'	–	3618	3597	3806	3453	(N–H) υ	54
5	A'	3415m	3527	3507	3805	3452	(N–H) υ	100
6	A'	3323w	3236	3217	3380	3066	(C–H) υ	96
7	A'	–	3228	3209	3376	3063	(C–H) υ	79
8	A'	–	3220	3201	3368	3055	(C–H) υ	96
9	A'	–	3214	3196	3360	3048	(C–H) υ	81
10	A'	–	3211	3193	3356	3044	(C–H) υ	73
11	A'	–	3193	3175	3338	3028	(N–H) υ	96
12	A'	–	3191	3173	3337	3027	(C–H) υ	86
13	A'	3157vs	3184	3166	3321	3013	(C–H) υ	95
14	A'	–	1774	1764	1920	1742	(O=C) υ	79
15	A'	–	1772	1762	1914	1736	(O=C) υ	78
16	A'	–	1674	1664	1822	1653	(C=C) υ	18
17	A'	1656vs	1671	1661	1795	1628	(C=C) υ	20
18	A'	–	1644	1634	1780	1614	(C–C) υ	19
19	A'	–	1633	1623	1774	1609	(C–C) υ	28
20	A'	–	1622	1612	1772	1607	(N–H) δ	75
21	A'	1604s	1620	1610	1761	1597	(N–H) δ	76
22	A'	–	1578	1569	1750	1587	(N–N) υ	25
23	A'	–	1561	1552	1696	1538	(N–N) υ	47
24	A'	1525s	1542	1533	1671	1516	(H–C) δ	17
25	A'	–	1519	1510	1652	1498	(H–N) δ	22
26	A'	–	1455	1446	1556	1411	(C–C) υ	27
27	A'	–	1453	1444	1551	1407	(C–C) υ	24
28	A'	1392vs	1389	1381	1473	1336	(N–C) υ	22
29	A'	–	1385	1377	1471	1334	(N–C) υ	21
30	A'	–	1373	1365	1455	1320	(C–C) υ	11
31	A'	–	1369	1361	1443	1309	(C–C) δ	12
32	A'	–	1336	1328	1380	1252	(H–C) δ	31
33	A'	1307m	1325	1317	1340	1215	(C–H) δ	26
34	A'	1275vs	1287	1279	1333	1209	(H–N) δ	25
35	A'	–	1267	1259	1294	1174	(H–N) δ	38
36	A'	–	1240	1233	1286	1166	(N=N) υ	32
37	A'	1199vs	1198	1191	1282	1163	(H–C) δ	28
38	A'	1168vs	1186	1179	1266	1148	(C–H) δ	28
39	A'	–	1155	1148	1233	1118	(C–C) υ	17
40	A'	–	1153	1146	1232	1117	(C–C) υ	18
41	A'	–	1139	1132	1195	1084	(C–H) δ	25
42	A'	–	1133	1126	1186	1076	(C–H) δ	17
43	A'	–	1095	1088	1180	1070	(H–N) δ	43
44	A'	–	1094	1087	1175	1066	(H–N) δ	43
45	A'	–	1033	1027	1109	1006	(C–C) δ	41
46	A'	–	1031	1025	1105	1002	(C–C) δ	37
47	A''	–	1003	997	1101	998	(CC) τ	46
48	A''	–	988	982	1099	997	(CC) τ	61
49	A''	–	974	968	1081	980	(CC) τ	43
50	A''	–	970	964	1079	978	(CC) τ	50

Table 2. (Contd.)

No.	Symmetry species C_S	Observed frequency	Calculated frequency				Vibrational assignments	PED, %
		FT-IR	PBE1PBE/6-31+G(2*d*,*p*)		HF/6-311+G(2*d*,*p*)			
			unscaled	scaled	unscaled	scaled		
51	A'	–	960	954	1019	924	(N–N) δ	15
52	A''	–	883	878	970.4	880	(CC) τ	33
53	A''	–	861	856	943.4	855	(CC) τ	27
54	A'	850s	856	851	937.5	850	(C–C) δ	12
55	A''	–	847	842	915.3	830	(CC) τ	32
56	A''	–	831	826	901.2	817	(CC) τ	37
57	A''	–	792	787	866.9	786	(NC) γ	37
58	A''	779s	783	778	859.7	780	(NC) γ	39
59	A'	–	780	775	830.0	753	(C–C) υ	10
60	A'	725m	732	727	782.2	709	(C–C) υ	10
61	A''	–	718	713	779.6	707	(C–C) τ	26
62	A''	–	715	710	776.0	704	(C–C) τ	23
63	A'	–	648	644	697	632	(C–C) δ	15
64	A'	–	638	634	690	626	(OCN) δ	21
65	A''	–	632	628	680	616	(C–C) γ(C–N) γ	13
66	A''	613m	629	625	622	564	(N–N) τ	85
67	A'	567m	576	572	602	546	(CN) δ	14
68	A''	–	558	554	593	538	(N–C) τ	38
69	A''	–	548	544	561	508	(N–C) τ	54
70	A''	–	523	520	559	507	(N–C) τ	23
71	A'	–	513	510	539	489	(NCC) δ	21
72	A''	–	491	488	531	481	(NCC) δ	32
73	A''	–	483	480	514	466	(C–C) γ	21
74	A''	–	444	441	475	430	(NCC) γ	12
75	A''	–	422	419	461	418	(C–C) τ	23
76	A''	–	418	415	455	412	(C–C) τ	32
77	A'	–	409	406	439	398	(C–N) δ	17
78	A''	–	380	377	438	397	(N–C) τ	68
79	A''	–	377	374	435	394	(N–C) τ	68
80	A''	–	341	339	370	335	(N–C) τ	16
81	A''	–	340	338	363	329	(N–N) τ	11
82	A''	–	286	284	301	273	(C–C) γ	25
83	A'	–	249	247	269	244	(CCC) δ	16
84	A'	–	218	216	235	213	(CCC) δ	16
85	A''	–	216	214	232	210.	(N–N) τ	26
86	A'	–	178	177	189	171	(CCC) δ	14
87	A''	–	173	172	155	140	(N–N) τ	40
88	A'	–	126	125	136	123	(NCC) δ	19
89	A''	–	113	112	112	101	(C–C) τ	24
90	A''	–	63	63	69	62	(C–C) τ	77
91	A''	–	63	62	67	60	(C–C) τ	64
92	A''	–	57	56	56	50	(C–C) τ	22
93	A'	–	35	35	36	32	(NNC) δ	26
94	A''	–	25	25	18	16	(N–C) τ	56
95	A''	–	9	9	8	7	(C–C) τ	68
	a			0.997		0.958		
	b			5.992		14.04		
	R^2			0.998		0.996		

$Freq_{exp} = aFreq_{theo} + b$.

vs—very strong; s—strong; m—medium; w—weak; υ—stretching; δ—in plane bending; γ—out plane bending; τ—torsion.

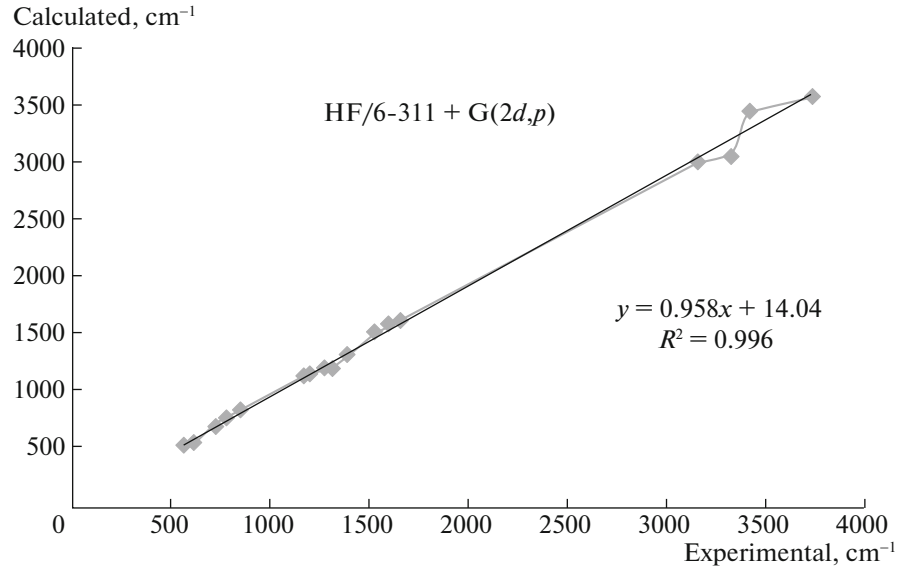

Fig. 5. Correlation between the experimental and computed frequencies of BBT.

in the FT-IR spectrum is 1656 cm^{-1} and it has been assigned to C=C stretching vibration (mode no. 17) with the contribution of 20%. The theoretically computed value, PBE1PBE/6-311+G(2*d*,*p*), at 1661 cm^{-1} shows satisfactory agreement with experimental value. Besides, the ring C=C stretching vibration is repressed as a result of the bonding of N=N in the ring.

3.2.3. C–C vibrations. The aromatic ring C–C vibrations usually occurs in the region of 1600–1400 cm^{-1} [37, 38]. In the present case, the C–C stretching vibrations have been assigned 725 (mode no. 60) that involves the contribution of 10%. Corresponding near calculated frequency is 727 cm^{-1} with RPBE1PBE/6-311+G(2*d*,*p*) method. When compared to the literature range cited above all bands are missing, which is due to the strong coupling of N=N between the ring and worsening with the increase of mass of substitutions. The strong band presented at 850 cm^{-1} assigned to CCC in-plane bending (mode no. 54) with the contribution of 12%.

These assignments are according to the assignments suggested by the literature [39].

3.2.4. N=N and N–N vibrations. Azo moieties are non-polar in nature, therefore they do not have obvious peaks in IR spectroscopy and their recognition is difficult [40–42]. On the other hand, the weak absorption of azo group falls in the same region as the absorption of aromatic compounds. Thus, for title compound, we cannot observe N=N stretching, N–N stretching, N=N–N-ring in-plane. Only N–N out-of-plane bending vibration is at 613 cm^{-1} (mode no. 66). Corresponding near calculated frequency is 625 cm^{-1} with RPBE1PBE/6-311+G(2*d*,*p*) method. As indicated by the PED, these modes (modes no. 66) involve the contribution of 85%.

3.2.5. N–H and C–N vibrations. FT-IR spectrum of BBT has very strong band at 3606 cm^{-1} assigned to N–H stretching vibration. The theoretical wavenumber of N–H stretching vibration (mode no. 3) 3529 cm^{-1} matches very well with the experimental value. The PED confirms that this mode of vibration is pure as it does not combine with any other mode.

Because of the combining of several probable bands in this region, the identification of C–N vibrations is very challenging. Sundaraganesan et al. [43] determined C–N stretching absorption in 1382–1266 cm^{-1} for aromatic amines. In benzamide, the observed band at 1368 cm^{-1} is assigned to C–N stretching [44]. Hence the strong band is observed at 1392 for C–N stretching vibrations (mode no. 28). The observed band at 779 cm^{-1} is related to C–N out of plan bending (mode no. 58). The theoretically scaled wavenumbers obtained at 1381 and 778 cm^{-1} by RPBE1PBE/6-311G+(2*d*,*p*) method. As indicated by the PED, these modes (mode nos. 28 and 58) involve the contribution of 22 and 39%.

All the vibrations are shifted down due to the suppression of N=N.

3.2.6. $CONH_2$ vibrations. In present study, the C=O stretching vibration is observed at 3157 cm^{-1} (mode no. 13). The PED of this mode involves the contribution of 95%. The computed wavenumber for the same mode at 3166 cm^{-1} is in good agreement with the experimental value. The NH_2 group has two N–H stretching vibrations, one being asymmetric and the other symmetric. The frequency of asymmetric vibration is greater than symmetric one. The strong bands

Table 3. Observed and calculated NMR chemical shifts (ppm) for 1,3-bis(4-amidophenyl)triazene obtained using ACD/NMR and Gaussian programs

Atom	Exp.	ACD/NMR	$\Delta\delta^a$	Gaussian			
				PBE1PBE/6-311+(2*d*,*p*)	$\Delta\delta^b$	HF/6-311+(2*d*,p)	$\Delta\delta^c$
C1	116.45	116.85	−0.4	111.61	4.84	111.64	4.81
C2	128.34	132.15	−3.81	129.01	−0.67	139.03	−10.69
C3	124.61	127.98	−3.37	129.10	−4.49	129.37	−4.76
C4	128.39	132.15	−3.76	134.41	−6.02	144.15	−15.76
C5	116.41	116.85	−0.44	114.40	2.01	115.14	1.27
C6	146.54	150.34	−3.8	143.79	2.75	154.54	−8
C10	154.35	152.36	1.99	153.08	1.27	157.90	−3.55
C11	120.79	122.14	−1.35	128.81	−8.02	131.68	−10.89
C12	127.60	128.9	−1.3	127.27	0.33	134.76	−7.16
C13	130.99	131.62	−0.63	133.97	−2.98	137.99	−7
C14	127.60	128.9	−1.3	133.51	−5.91	139.69	−12.09
C15	120.69	122.14	−1.45	116.38	4.31	120.31	0.38
C16	168.16	168.66	−0.5	167.54	0.62	173.14	−4.98
C30	168.16	168.66	−0.5	166.70	1.46	173.02	−4.86
H26N	3.32	7.22	−3.9	5.21	−1.89	4.68	−1.36
H27N	3.32	7.22	−3.9	6.04	−2.72	4.87	−1.55
H33N	3.34	7.22	−3.88	5.25	−1.91	4.59	−1.25
H34N	3.34	7.22	−3.88	5.90	−2.56	4.79	−1.45
H28N	12.84	8.75	4.09	10.01	2.83	9.23	3.61
H19A	7.30	7.71	−0.41	8.95	−1.65	8.31	−1.01
H20A	7.41	8.17	−0.76	8.69	−1.28	8.57	−1.16
H21A	7.40	8.17	−0.77	9.50	−2.1	9.31	−1.91
H22A	7.60	8.07	−0.47	8.61	−1.01	8.40	−0.8
H23A	7.93	7.93	0	8.72	−0.79	8.51	−0.58
H24A	7.93	7.93	0	9.49	−1.56	9.20	−1.27
H25A	7.92	8.07	−0.15	9.18	−1.26	8.57	−0.65
H29A	7.29	7.71	−0.42	7.78	−0.49	7.36	−0.07

[a] $\delta_{exp} - \delta_{ACD/NMR}$, [b] $\delta_{exp} - \delta_{B3LYP/6\text{-}311++G(d,p)}$, [c] $\delta_{exp} - \delta_{HF/6\text{-}311++G(d,p)}$.

observed at 3732 and 3415 cm^{-1} are assigned to asymmetric and symmetric stretching vibrations, respectively. According to this observation, the theoretically scaled wavenumbers, 3723 and 3507 cm^{-1} by RPBE1PBE/6-311+G(2*d*,*p*) method are allotted to amino asymmetric and symmetric stretching vibrations, respectively (mode nos. 2 and 5). As indicated by the PED, these modes involve the contribution of 58 and 100%.

All the mentioned assignments are in excellent agreement with the literature [45, 46].

3.3. NMR Spectroscopy

The molecular structure of BBT was optimized. Then, gauge including atomic orbital (GIAO) NMR chemical shifts calculations of the title compound had been carried out using RPBE1PBE/6-311+G(2*d*,*p*) and HF/6-311+G(2*d*,*p*) levels. The GIAO method is one of the most common approaches for calculating isotropic nuclear magnetic shielding tensors [47, 48]. Moreover, the NMR spectra calculations were estimated by using the ACD/NMR software. The third column of Table 3 included ACD calculated shifts. According to these data and comparing the correla-

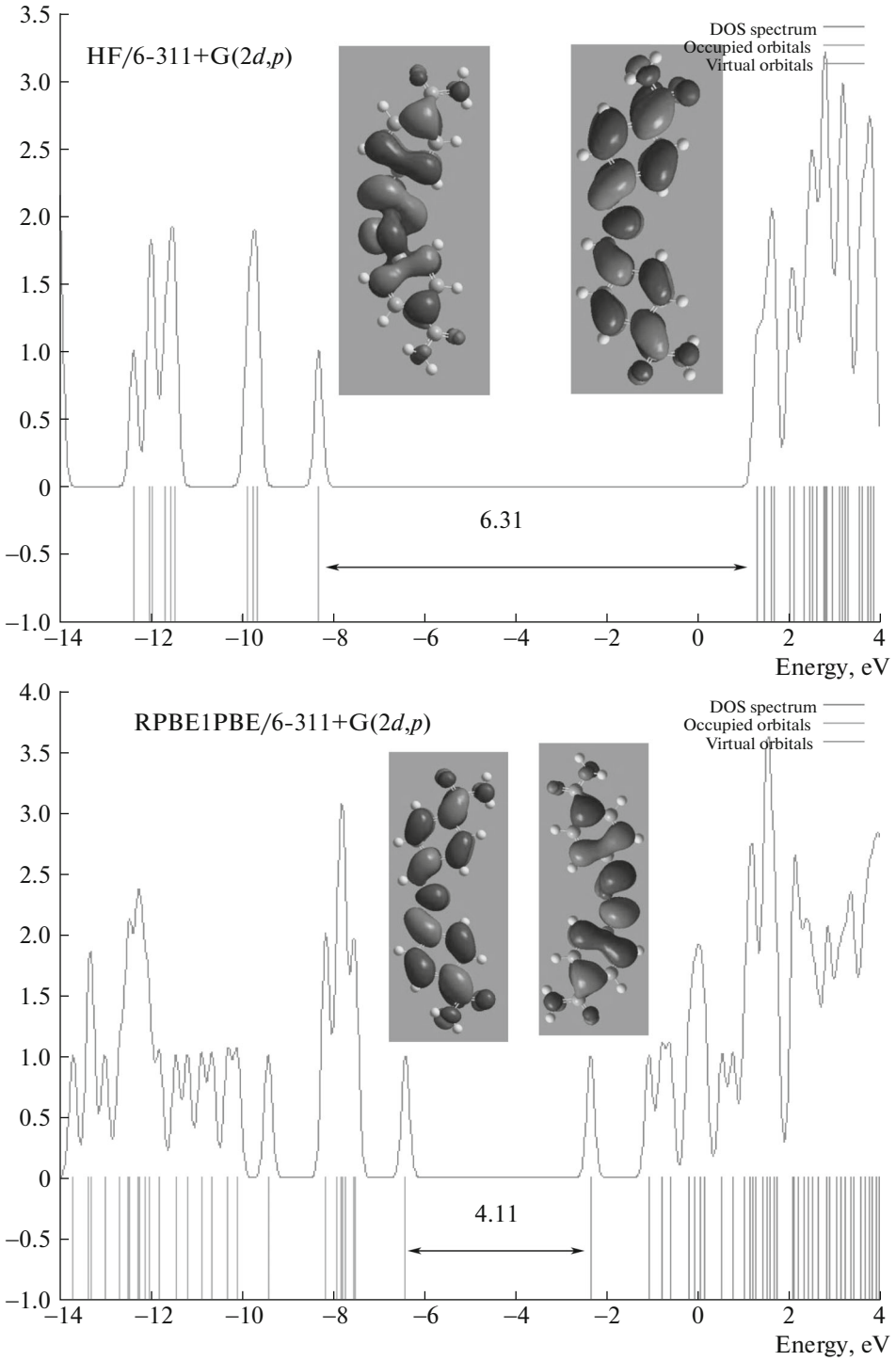

Fig. 6. Partial DOS diagram contain HOMO (left) and LUMO (right) plot of BBT.

tion coefficient values, it is seen that the results of ACD/NMR are closer to experimental data compared to other calculated methods. The phenyl protons resonate as the multiplet at 7.29–7.93 ppm experimentally and these have been predicted in the range 7.78–9.50 ppm at RPBE1PBE/6-311+G(2*d*,*p*), 7.36–9.31 ppm at HF/6-311++G(*d*,*p*) and 7.71–8.17 ppm at ACD/HNMR. The singlet observed at 12.84 ppm is assigned to H3N and this has been computed to be in 10.01, 9.23, 8.75 ppm at RPBE1PBE/6-311+G(2*d*,*p*), HF/6-311+G(2*d*,*p*), and ACD/HNMR, respectively. Complete ^{1}H NMR chemical shifts are listed in Table 3. The signals in the range 116.41 and 146.54 ppm are assigned to C1–C6 atoms and the

Table 4. Theoretically computed total energies (kcal mol^{-1}), zero-point vibrational energies (kcal mol^{-1}), rotational constants (GHz), entropies (kcal mol^{-1}), enthalpies (kcal mol^{-1}), Gibbs free energies (kcal mol^{-1}), dipole moment (Debye), and some physico-chemical properties of BBT

Parameters	RPBE1PBE/6-311+G(2*d*,*p*)	HF/6-311+G(2*d*,*p*)
Total energy	−605352.387	−602374.874
Zero−point energy	−605175.432	−602199.658
Rotational constants	1.1407	1.1397
	0.0836	0.0838
	0.0781	0.0782
Entropy		
Total	146.716	144.135
Translational	42.820	42.820
Rotational	35.022	35.017
Vibrational	68.875	66.298
Enthalpy	−605175.432	−602187.905
Gibbs free energy	−605218.73	−602230.575
Dipole moment (D)		
X	1.4620	1.8722
Y	−1.4711	−1.4493
Z	0.3043	0.5583
Total	2.0963	2.4326
Properties		Values
Molar Refractivity[a] (cm^3)		76.66 ± 0.5
Molar Volume[a] (cm^3)		203.2 ± 7.0
Parachor[a] (cm^3)		570.2 ± 8.0
Index of refraction[a]		1.678 ± 0.05
Surface tension[a] (dyne/cm)		61.9 ± 7.0
Density[a] (g/cm^3)		1.39 ± 0.1
Polarizability[a] (cm^3)		30.39 ± 0.5 × 10^{-24}
log*P*		1.8[b]
		−0.21[c]
		1.82[d] ± 0.53

[a] ACD/ChemSketch, [b] ChemBioOffice Ultra, [c] HyperChem, [d] ACD/log*P*.

computed values at ACD/CNMR level are in the range 116.85−150.34 ppm. The results of ^{13}C NMR calculations are listed in Table 3.

3.4. HOMO−LUMO Energy

Both the highest occupied molecular orbital (HOMO) and the lowest unoccupied molecular orbital (LUMO) are the most important orbitals participating in chemical reaction. The HOMO energy describes the ability of electron donating, the LUMO shows the ability of electron withdrawing, and the gap between HOMO and LUMO indicates the molecular chemical stability [49]. In the frontier region, neighboring orbitals are being with short distance. In these cases, consideration of the HOMO and LUMO singly may not yield a realistic description of the frontier orbitals. Hence, the density-of-states (DOS) in terms of Mulliken population analysis were calculated using the GaussSum program. The DOS diagram is presented in Fig. 6. The DOS plot mainly provides the combination of the fragment orbitals that are partnership in molecular orbitals. The HOMO−LUMO energy gap of BBT was obtained at the RPBE1PBE/6-311+G(2*d*,*p*) level, which demonstrates the chemical activity of the molecule. The calculated energies and the energy gap is HOMO = −6.6, LUMO = −2.49, and HOMO−LUMO energy gap = 4.11 eV. The energy gap (4.11 eV) of HOMO−LUMO explains the probable charge transfer interaction within the molecule affecting the biological activity of the molecule.

3.5. Molecular Electrostatic Potential Maps

The calculated molecular electrostatic potential (MESP) is an effective tool in many fields such as chemistry. The MESP widely used for prediction most probable regions for the electrophilic attack of charged point-like reagents on organic molecules [50, 51]. With the purpose of charge distribution determination in the molecule and prediction the reactive sites for electrophilic and nucleophilic attacks of BBT, MESP was calculated at the HF/6-311+G(2*d*,*p*) and RPBE1PBE/6-311+G(2*d*,*p*) levels (Fig. 1). The negative regions of MESP were related to electrophilic reactivity and the positive ones to nucleophilic reactivity. As depicted in Fig 1, this molecule has two possible sites for electrophilic attack. The negative regions are mainly over the C11 and the partial region in the middle of N7, C6, and C5 atoms.

3.6. Calculated Thermodynamic and Physico-Chemical Properties

Several thermodynamic factors calculated by HF/6-311+G(2*d*,*p*) and RPBE1PBE/6-311+G(2*d*,*p*) basis sets have been given in Table 4. Scale factors have been recommended for an accurate prediction determining zero-point vibrational energies for calculations [51]. The total energy of the molecule was the sum of the translational, rotational, vibrational and electronic energies. The zero point vibrational energy of the BBT at HF/6-311+G(2*d*,*p*) and RPBE1PBE/6-311+G(2*d*,*p*) levels were −602199.658 and −605175.432 kJ mol^{-1}, respectively. The logarithm of the partition coefficient for *n*-octanol/water (log*P* values) of the BBT was calculated using three commercially available software (ChemBioOffice Ultra 11.0 [52], ACD/LogP [24], and ALOGPS [53−55]). The

log *P* is one criterion used in medicinal chemistry to assess the druglikeness of a given molecule and used to calculate lipophilic efficiency, a function of potency and log *P* that evaluates the quality of research compounds [56, 57]. The log *P* value is also known as a measure of lipophilicity. For comparison, the log *P* was higher than *p*-dichlorobenzene and lower than 2,2',4,4',5-pentachlorobiphenyl.

CONCLUSIONS

The title compound was synthesized via reaction of 4-aminobenzamide and sodium nitrite in acidic solution. The structure was determined and characterized by FT-IR, ^{1}H, and ^{13}C NMR. The molecular geometries, harmonic vibrational frequencies, chemical shifts, MESP and thermodynamic properties of BBT are determined and analyzed by HF and DFT (RPBE1PBE) with 6-311+G(2*d*,*p*) basis set. Comparison between the calculated optimized geometry and the experimental values indicates that the RPBE1PBE/6-311+G(2*d*,*p*) method can predict the bond length, bond angle and dihedral angles of the BBT better than HF/6-311+G(2*d*,*p*) method. The calculated vibrational wavenumbers and the experimental FT-IR spectrum agreeably support each other. The difference between the observed and scaled wavenumber values of most of fundamentals is very small. Comparison between the calculated and experimental chemical shifts indicates that ACD/NMR result is closer to the experimental frequencies than DFT and HF methods. The MESP study shown negative regions are mainly over the C11 and the partial region in the middle of N7, C6, and C5 atoms. The log *P* was higher than *p*-dichlorobenzene and lower than 2,2',4,4',5-pentachlorobiphenyl.

ACKNOWLEDGMENT

The authors would like to thank Tabriz Branch, Islamic Azad University for the financial support of this research, which is based on a research project contract.

REFERENCES

1. P. Griess, Proc. R. Soc. London **9**, 594 (1859).
2. D. Enders, C. Rijksen, E. B. Köbberling, A. Gillner, and J. Köbberling, Tetrahedron Lett. **45**, 2839 (2004).
3. M. K. Rofouei, E. Fereyduni, J. A. Gharamaleki, G. Bruno, and H. A. Rudbari, Acta Crystallogr. E **66**, m1082 (2010).
4. E. Fereyduni, M. K. Rofouei, M. Kamaee, S. Ramalingam, and S. M. Sharifkhani, Spectrochim. Acta A **90**, 193 (2012).
5. M. K. Rofouei, J. A. Gharamaleki, E. Fereyduni, A. Aghaei, G. Bruno, and H. A. Rudbari, Z. Anorg. Allg. Chem. **638**, 220 (2012).
6. M. Horner, V. F. Giglio, A. J. R. W. A. Santos, A. B. Westphalen, B. A. Iglesias, P. R. Martins, C. H. Amaral, T. M. Michelot, L. G. B. Reetz, C. M. Bertoncheli, G. L. Paraginski, and R. Horner, Rev. Bras. Cienc. Farmaceut. **443**, 441 (2008).
7. A. J. R. W. A. Santos, R. Horner, G. L. Paraginski, F. C. Machado, and M. Horner, Anal. Sci. **23**, x251 (2007).
8. A. Katsoulas, Z. Rachid, F. Brahimi, J. Mcnamee, and C. B. J. Jean, Leuk. Res. **29**, 693 (2005).
9. M. Sanada, Y. Takagi, R. Ito, and M. Sekiguchi, DNA Repair **3**, 413 (2004).
10. F. Barcelo and M. O. Lombardia, J. Portugal Biochim. Biophys. Acta. **1519**, 175 (2001).
11. B. A. Iglesias, M. Horner, H. E. Toma, and K. Araki, J. Porphyr. Phthalocyan. **16**, 200 (2012).
12. G. M. Oliveira, M. Horner, A. Machado, M. A. Villetti, D. F. Back, and A. Iglesias, J. Mol. Struct. **928**, 85 (2009).
13. G. M. Oliveira, M. Horner, A. Machado, D. F. Back, J. H. S. K. Monteiro, and M. R. Davolos, Inorg. Chim. Acta. **366**, 203 (2011).
14. F. Feng, X. Liao, Z. Chen, S. Lin, S. Meng, and Z. Lu, Anal. Chim. Acta. **575**, 68 (2006).
15. S. Ressalan and C. S. P. Iyer, J. Lumin. **111**, 121 (2005).
16. A. J. dos Santos, P. Bersch, H. P. M. de Oliveira, M. Horner, and G. L. Paraginski, J. Mol. Struct. **1060**, 264 (2014).
17. D. B. Kimball, R. Herges, and M. M. Haley, J. Am. Chem. Soc. **124**, 1572 (2002).
18. P. Zhao, Z. Zhang, P. J. Wang, and D. S. Liu, Physica B **404**, 3462 (2009).
19. P. J. Martin, *Introduction to Molecular Electronics* (Oxford University Press, New York, 1995).
20. M. Taniguchi, M. Uehara, and Y. Katsura (Seiko Epson Corp.), Jpn. Kokai Tokkyo JP **05 01**, 007 (1993).
21. H. Khani, M. K. Rofouei, P. Arab, V. K. Gupta, and Z. Vafaei, J. Hazard. Mater. **183**, 402 (2010).
22. M. J. Frisch, G. W. Trucks, H. B. Schlegel, G. E. Scuseria, M. A. Robb, J. R. Cheeseman, J. A. Montgomery, T. Vreven, K. N. Kudin, J. C. Burant, J. M. Millam, S. S. Iyengar, J. Tomasi, V. Barone, B. Mennucci, et al., *Gaussian 03 Revision C.02* (Gaussian Inc., Pittsburgh, PA, 2003).
23. P. J. Merrick, D. Moran, and L. Radom, J. Phys. Chem. A **111**, 11683 (2007).
24. Advanced Chemistry Development, Inc., ACD/HNMR and ACD/CNMR. http://www.acdlabs.com
25. N. M. O'Boyle, A. L. Tenderholt, and K. M. Langner, J. Comput. Chem. **29**, 839 (2008).
26. V. O. Domingues, R. Horner, L. G. B. Reetz, F. Kuhn, V. M. Coser, J. N. Rodrigues, R. Bauchspiess, W. V. Pereira,G. L. Paraginski, A. Locatelli, J. O. Fank, V. F. Giglio, and M. Horner, J. Braz. Chem. Soc. **21**, 2226 (2010).
27. M. R. Melardi, M. Aghamohamadi, J. A. Gharamaleki, M. K. Rofouei, and B. Notash, Acta Crystallogr. E **68**, o724 (2012).
28. Y. Erdogdu, M. T. Gulluoglu, and M. Kurt, J. Raman Spectrosc. **40**, 1615 (2009).

29. E. Fereyduni, E. Vessally, E. Yaaghubi, and N. Sundaraganesan, Spectrochim. Acta, Part A **81**, 64 (2011).
30. G. Keresztury, in *Handbook of Vibrational Spectroscopy*, Ed. By J. M. Chalmers and P. R. Griffiths (Wiley, New York, 2002), Vol. 1, p. 71.
31. V. Krishnakumar, N. Prabavathi, and S. Muthunatesan, Spectrochim. Acta A **70**, 991 (2008).
32. C. Lee, W. Yang, and R. G. Parr, Phys. Rev. B **37**, 785 (1988).
33. A. D. Becke, J. Chem. Phys. **98**, 5648 (1993).
34. N. P. G. Roeges, *A Guide to the Complete Interpretation of Infrared Spectra of Organic Structures* (Wiley, New York, 1994).
35. E. Vessally, E. Fereyduni, Y. Erdogdu, A. Habibi, K. Eskandari, and M. T. Gulluoglu, J. Mol. Struct. **985**, 120 (2011).
36. G. Varsanyi, *Vibrational Spectra of Benzene Derivatives* (Academic Press, New York, 1969).
37. Z. Asadi, M. B. Asnaashariisfahani, E. Vessally, and M. D. Esrafili, Spectrochimi. Acta A **140**, 585 (2015).
38. S. Ramalingam, P. D. S. Babu, S. Periandy, and E. Fereyduni, Spectrochim. Acta Part A **84**, 210 (2011).
39. H. AbdelShafy, H. Perlmutter, and H. Kimmel, J. Mol. Struct. **42**, 37 (1977).
40. L. Clougherty, J. Sousa, and G. Wyman, J. Org. Chem. **22**, 462 (1957).
41. R. Kubler, R. W. Luttke, and S. Weckherlin, Z. Electrochem. **64**, 650 (1960).
42. K. J. Morgan, J. Chem. Soc., 2151 (1961).
43. N. Sundaraganesan, J. Karpagam, S. Sebastian, and J. P. Cornard, Spectrochim. Acta A **73**, 11 (2009).
44. R. Shunmugam and D. N. Sathyanarayana, Spectrochim. Acta A **40**, 757 (1984).
45. N. P. G. Roeges, *A Guide to the Complete Interpretation of Infrared Spectra of Organic Structures* (Wiley, New York, 1994).
46. A. S. ElShahawy, S. M. Ahmed, and N. K. Sayed, Spectrochim. Acta A **66**, 143 (2007).
47. R. Ditchfield, J. Chem. Phys. **56**, 5688 (1972).
48. K. Wolinski, J. F. Hilton, and P. Pulay, J. Am. Chem. Soc. **112**, 8251 (1990).
49. K. Fukui, Science **218**, 747 (1982).
50. P. Politzer and D. G. Truhlar, *Chemical Application of Atomic and Molecular Electrostatic Potentials* (Plenum, New York, 1981).
51. C. A. Hunter, Angew. Chem. Int. Ed. **43**, 5310 (2004).
52. ChemBioDraw Ultra, Version 11.0, CambridgeSoft
53. I. V. Tetko, J. Gasteiger, R. Todeschini, A. Mauri, D. Livingstone, P. Ertl, V. A. Palyulin,; E. V. Radchenko, N. S. Zefirov, A. S. Makarenko, and V. Y. Tanchuk, J. Comput. Aid Mol. Des. **19**, 453 (2005).
54. VCCLAB, Virtual Computational Chemistry Laboratory (2005). http://www.vcclab.org
55. I. V. Tetko, Drug Discov. Today **10**, 1497 (2005).
56. M. P. Edwards and D. A. Price, Ann. Rep. Med. Chem. **45**, 381 (2010).
57. P. D. Leeson and B. Springthorpe, Nat. Rev. Drug Discov. **6**, 881 (2007).
58. S. P. Wasik, Y. B. Tewari, M. M. Miller, and D. E. Martire, NBS Tech Rep **81**, 56 (1981).
59. J. Brodsky, K. Ballschmiter, and Z. Fresenius, Anal. Chem. **331**, 295 (1988).